Journal of Hazardous Materials Advances 7 (2022) 100135

Contents lists available at ScienceDirect

Journal of Hazardous Materials Advances

journal homepage: www.elsevier.com/locate/hazadv

Histopathological and ultrastructural alterations reveal the toxicity of particulate matter ($PM_{2.5}$) in adult zebrafish

Bangeppagari Manjunatha [a], Eunseok Seo [b], Deekshitha Bangyappagari [c], Sang Joon Lee [a,b,*]

[a] Center for Biofluid and Biomimic Research, Pohang University of Science and Technology (POSTECH), Pohang 37673, South Korea
[b] Department of Mechanical Engineering, Pohang University of Science and Technology (POSTECH), Pohang 37673, South Korea
[c] Gandhi Medical College, Secunderabad, Telangana 500003, India

ARTICLE INFO

Keywords:
Diesel particulate matter
Toxicity
Morphological damage
Multi-organs dysfunction
micro CT image
Zebrafish

ABSTRACT

The exposure of fine particulate matter ($PM_{2.5}$) can lead to developmental toxicity in organs. However, the underlying specific mechanisms are still unclear. Especially, the toxic effects of $PM_{2.5}$ on adult zebrafish are still obscure. In this study, for the first time, the toxic effects of $PM_{2.5}$ on zebrafish (*Danio rerio*) as well as the changes in cellular and subcellular traits of multi-organs were investigated. The treatment groups were exposed to 100 mg/L $PM_{2.5}$ for 5 days. The pathological and ultrastructural changes in multi-organs of the treatment and control (without $PM_{2.5}$) groups were subsequently examined. As a result, histopathological alterations were obviously noted the exposed multi-organs (gill, liver, intestine, heart and gonads) of adult zebrafish. Especially, marked changes were observed after the exposure of $PM_{2.5}$ in intestine images of X-ray micro CT. In addition, when typical ultrastructural arrangements of multi-organs (gill, liver and intestine) were examined, their contours were unclear, and organelles were dissolved, necrotized and almost degenerated in the treated zebrafish group. These adverse effects of $PM_{2.5}$ on multi-organs might raise a potential concern for zebrafish development and reproduction. Furthermore, these multi-organ alterations could be used as a sensitive biomarker in the toxicity assessment of $PM_{2.5}$. In addition, the present results would be useful for better understanding of $PM_{2.5}$-induced toxicity to organisms, and the cellular and subcellular impairments in multi-organs may affect aquatic organisms.

Introduction

Global air pollution becomes a major public health concern, particularly in developing countries. The World Health Organization (WHO) reported that about 91% of the world's population live in areas that fail to meet its air quality guidelines (WHO, 2018a). Air pollution has been considered as the greatest environmental risk to human health by the WHO, responsible for more than 7 million annual premature deaths worldwide (WHO, 2019). Particulate matter (PM) might be the most important pollutant to human, compared to any other pollutants (WHO, 2018b).

Air pollutants adversely affects human health. Recently, particulate matter (PM), ozone (O_3) and nitrogen dioxide (NO_2) are the leading pollutants in urban environment. Harmful ambient toxins in the atmosphere is the main reason of concern (Lelieveld et al., 2015). As validated in a previous work, the polluted air is highly responsible for various ailments associated with lungs, heart and gonads (Darrow et al., 2014; Hu et al., 2014; Zhou et al., 2014). Such ailments include the impairment of biological functions and may trigger tumor formation in respective organs (Darrow et al., 2014; Hu et al., 2014; Zhou et al., 2014). Previous epidemiological studies established a correlation between the increase in respiratory and cardiovascular diseases and PM concentration of the surrounding air (Lee et al., 2014; Du et al., 2016). Similarly, PM exposure induces reactive oxidative stress (ROS) (Park et al., 2018), inflammation (Wang et al., 2017), mitochondrial dysfunction (Chew et al., 2020), and autophagy (Fu et al., 2017). Due to increased air pollution, the health of population in Chinese big cities has taken high risk (Li et al., 2018; Hu and Guo, 2021). On average, 1.3 billion Chinese are exposed to PM, far beyond the WHO air quality guidelines (Song et al., 2017). The air pollution caused by PM enhances pulmonary and systemic oxidative stress, hypoxemia, induces immunological modifications, atherosclerosis, and chronic obstructive pulmonary disease (Carey et al., 2013; Lu et al., 2015). In some cases, the PM exposure was reported to the responsible for diabetes mellitus (Zanobetti et al., 2014).

A previous study established a strong association between long-term exposure to PM and hypertension (Yang et al., 2018). Similarly, several other studies focused to establish a relationship between the $PM_{2.5}$ exposure and myocardial infarction, arrhythmia, fibrillation and hypertension (Burgan et al., 2010). The exposure of $PM_{2.5}$ adversely affects the cardiovascular system through systemic inflammation and hyperco-

* Corresponding author.
E-mail address: sjlee@postech.ac.kr (S.J. Lee).

https://doi.org/10.1016/j.hazadv.2022.100135
Received 29 April 2022; Received in revised form 23 July 2022; Accepted 24 July 2022

agulability (Lippi et al., 2008; Chuang et al., 2007; Delfino et al., 2009). However, the evidence for the corresponding time course is limited.

Our previous studies demonstrated the acute toxicity effects of $PM_{2.5}$ on early embryonic development of zebrafish. However, little information is available on studies on adult zebrafish. Zebrafish have been commonly used as a model organism for studies of functional diseases and toxicity, as they are reported to have numerous advantages over other animal models (Dooley and Zon, 2000). For example, the upkeep of zebrafish is easier and cheaper than that of other animal models because of their small size, rapid development, and remarkable fertilization rate (Ali et al., 2011). Zebrafish are also a remarkable genetic model because of their genetic similarity to mammals, including humans; moreover, the genetic modification of zebrafish is relatively easy. As vertebrates, the major organs and tissues of zebrafish such as muscles, blood, intestines, kidneys, liver, and eyes are similar to those in humans (Chhetri et al., 2014; Wang et al., 2010). Therefore, zebrafish are useful for drug screening (Cassar et al., 2020).

The main objective of this study is to determine the potential toxicity of $PM_{2.5}$ in multi-organs of adult zebrafish. For this, the damages related to pathological and ultrastructural changes in multi-organs (gill, liver, intestine, heart and gonads) were assessed. Knowledge of pathological findings associated with $PM_{2.5}$ could help with a better understanding of pathogenic mechanisms, and more precise knowledge on the reversibility of multi-organs dysfunctions.

Materials and methods

Maintenance of zebrafish

Wild type zebrafish embryos were provided from the Zebrafish Center for Disease Modeling (ZCDM, Korea). We maintained zebrafish embryos in our laboratory for more than one year under the defined environmental conditions as described by Westerfield (1995). Adult male and female zebrafish with a mean total body length of 3.5 cm (± 0.5 SD) were obtained and stocked in de-chlorinated water (20 L). The obtained fish were acclimated for 5 days under constant aeration, 28 ˚C water temperature, 14 h:10 h (light: dark) cycle (Manjunatha and Philip, 2016). The system water was purified using 10- and 5-μm micro depth and activated-carbon filters. The pH of the system water was maintained between 6.8 and 7.5. If pH is lower than 6.8, it is adjusted by adding coral sand. They were fed twice daily with alternating diet of freshly hatched brine shrimp and commercial feed. All experiments using zebrafish samples were carried out according to the approved guidelines by the Animal Care and Ethics Committee of Pohang University of Science and Technology (POSTECH), South Korea (POSTECH-2019–0059).

Preparation of $PM_{2.5}$ particles

In this study, diesel particulate matter (DPM) NIST 1650b was procured from Sigma-Aldrich, Inc. (St. Louis, MO, USA) as $PM_{2.5}$ particles. DPM is chemical mixture of more than 100 PAHs. A stock solution (100 mg/4 mL) was prepared in dimethyl sulfoxide (DMSO) and sonicated for 30 min to avoid agglomeration of the suspended $PM_{2.5}$ particles.

Experimental animal

One year old zebrafish were divided into 4 groups: two control groups of male and females (n = 20) and 2 PM treatment groups of male and females (n = 20). Zebrafish (n = 10 per group) were exposed to 100 mg/L of $PM_{2.5}$ concentration in system water with a total volume of 1.5 L for one to 5 days without feeding. The PM concentration was determined according to the survival rate with respect to the environmental PM concentrations and incubation time was analysed, whereas control group (n = 10 per group). The final concentrations were varied depending on experimental settings. For control counterparts, 0.1% DMSO without $PM_{2.5}$ component. Fish treatments were conducted in three parallel replicates. However, survival rate and male organs (except testis) data was not shown in this study due to there being no difference between male and female organs.

Histopathological studies

Histopathological analysis was performed after 5 days exposure to $PM_{2.5}$ on gills, liver, intestine, heart and gonads. Initially, the zebrafish samples including control and treatment groups (n = 5 per each group) were anesthetized by immersion in either an ice-water (4 ˚C or less) bath or 0.14 mg/mL tricaine and followed by dissection in order to visualize different above mentioned organs. All organs were fixed in 4% paraformaldehyde solution for 24 h at room temperature. The fixed tissues were dehydrated and embedded in paraffin, sectioned, and stained with hematoxylin and eosin (H&E). The sample slides were examined by using a CCD camera (QIMAGINGQ42286, Canada). Protocol was followed as mention in our previous report (Manjunatha et al., 2021).

X-ray micro CT image analysis

The glutaraldehyde and paraformaldehyde each 2% final volume was used to fix the both control and treatment groups of zebrafish samples (n = 5/each experiment group in three biological replicates in parallel). The fixation was carried for the period of 24 h at 4 ˚C followed by post fixing in osmium tetroxide buffer (1%). Incubation conditions are as same as that of the primary fixation. For sample dehydration different concentrations of ethanol were used. The dehydration was begun with 25% then, 50%, and 75%, and finally followed with 100%, in each concentration samples were incubated for at least 30 min to ensure proper dehydration. Sample immersed in 100% ethanol was transferred to one end sealed pipette tip and the other end was closed with a with a lid (Dow Corning, USA). As both the ends are sealed the chances of ethanol evaporation during analysis was minimized. All the procedures of sample preparation to image capturing and analysis were performed as mentioned by Lee et al. (2019) and Seo et al. (2020) with necessary modifications. The 3D morphological structures of zebrafish samples in the form of 3 Dimensional images were using synchrotron X-ray micro-CT at the 6C Biomedical imaging beamline of Pohang Accelerator Laboratory (PAL, Pohang, Korea). The images generated upon passing samples through X-ray beam (22 keV) were captured by the high-speed camera (PCO AG, Germany). The camera was placed exactly 100 mm behind the sample. For tomographic slice images the samples were immobilized on a rotary stage (ABRS-150 MP-M-AS, Aerotech, Inc., Pittsburgh, PA, USA). To obtain 3 dimensional CT images a rotary stage was rotated from 0 – 180˚ with an intervals of 0.2˚ Overall 901 projection images were captured in this study. Further, the Octopus software (inCT, Gent, Belgium) and Amira image analysis software (FEI, Hillsboro, OR, USA) were used for image reconstruction.

Ultrastructural studies

Transmission electron microscope (TEM) imaging for the control and treatment zebrafish samples (n = 5/each experiment group in three biological replicates in parallel) was performed using TEM (JEOL JEM-2200FS) of the National Institute for Nanomaterials and Technology, Pohang. Initially, the propylene oxide and Spurr's resin were used to dehydrate the samples. The sample slices of roughly about 90 to 120 nm thickness were stained with 2% uranyl acetate and Reynolds' lead citrate (MT-X, RMC, Tucson, AZ, USA). Finally, the stained sections were observed under TEM at 80 kV.

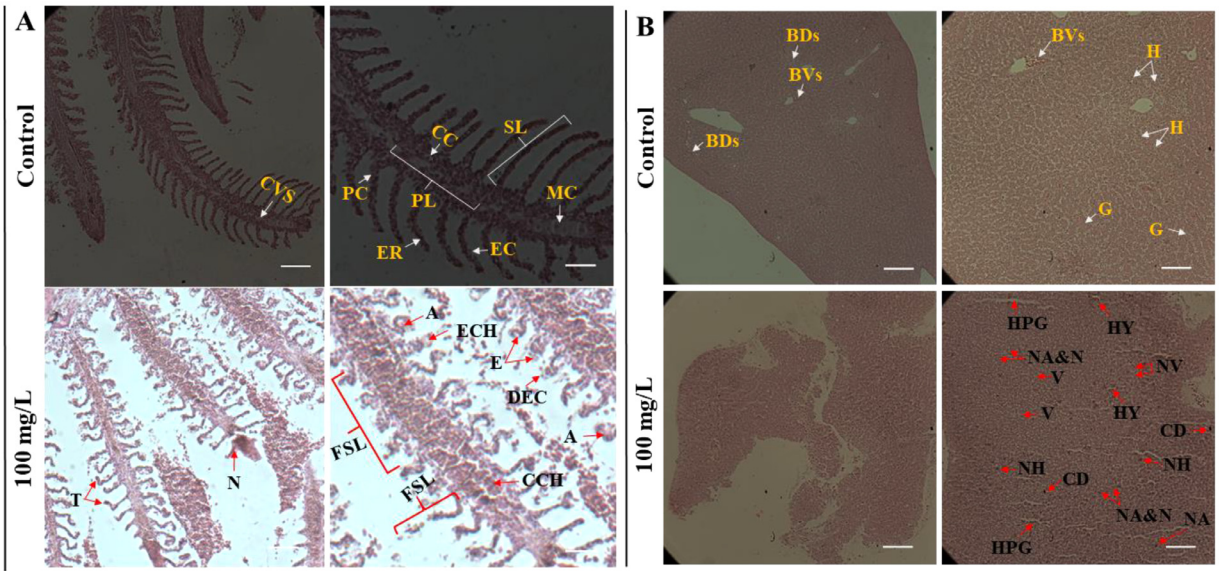

Fig. 1. Histopathological sections of the gills and liver female zebrafish stained with H&E. **(A)** The control gills show normal primary lamellae (PL), secondary lamellae (SL), chloride cells (CC), mucous cells (MC), epithelial cells (EC), erythrocytes (ER), pillar cells (PC) and cartilage supporting the venous sinusoids (CVS) (top side images). The $PM_{2.5}$ (100 mg/L) treated gills exhibit aneurysm (A), epithelial cell hyperplasia (ECH), edema (E), displacement of epithelial cells (DEC), chloride cell hyperplasia (CCH), necrosis (N), telangiectasis (T) and fusion of lamellae (FSL) (bottom side images). **(B)** The control liver shows hepatocytes (H), blood vessels (BVs), bile ducts (BDs) and glycogen (G) (top side images). The $PM_{2.5}$ treated liver exhibit hepatic plate gap (HPG), nucleus atrophy and necrosis of hepatocytes (NA&N), hyperemia (HY), vacuolization (V), nucleus vacuolization (NV), nucleus hypertrophy (NH) and cellular degeneration (CD) (bottom side images). Scale bar denotes 240 μm.

Results and discussion

Histopathology

Histopathological lesions have been used as important tools in biomonitoring and ecotoxicological studies due to ease interpretation, both in acute and chronic exposure situations (Santos et al., 2015). In this study, to evaluate the acute toxicity of $PM_{2.5}$ in zebrafish samples by waterborne exposure, the toxicological potential in multi-organs was elucidated at the histopathological and ultrastructural levels.

Histopathological changes in zebrafish gills

The morphology of zebrafish gills is similar to that of other freshwater Teleost, as reported by (Karlsson, 1983). The gills is highly sensitive to toxic compounds, and when exposed to them, it has typical tissue changes. One of the first alterations observed is the displacement of the lamella epithelial cells, which, according to Carvalho et al. (2018), can indicate an adaptation attempt in the aquatic animal to the ongoing new environmental conditions. The space between the lamellae and the displaced epithelial tissue is filled with water, forming edema, which can hamper the function of this organ, suffocating the animal (Campagna et al., 2008). The change in the function of the gills can lead to an increase in size in the epithelial cells (hyperplasia). As a consequence of hyperplasia, the fusion of secondary lamellae can occur (Meletti, 2016). This feature blocks the passage of water and blood to decrease the work overload of lamellae cells. However, it causes a deficit of oxygenation and can induce the death of the animal (Mazon et al., 2002). Chloride cells are located on the basis of secondary lamellae and are accountable to pump sodium and chloride ions into the fish to maintain its osmotic balance (Holden et al., 2012). Hence, hyperplasia in these cells may indicate an osmotic imbalance in the fish, as the organism tries to adapt through the increase of sodium and chloride transport into the blood to re-establish the homeostasis (Rezende et al., 2014).

Another essential cell in the maintenance of blood circulation is the pillar cell. Changes in its regular function can induce lamellae degeneration and blood flow dysregulation (Van Den Heuvel et al., 2000). Progressive distension of the pillar cells can cause aneurysms, hemorrhages, and gill tissue collapse through all lamellae (Carvalho et al., 2018). The histological examination of specific target organs is a valuable means for environmental monitoring, based on the established correlation between the test animal, and treatments. The histological results observed in multi-organs indicate that the $PM_{2.5}$ exposure causes major morphological changes in gills which perform respiration, detoxification, and osmoregulation, etc.

The gill sections observed by an optical microscope show normal morphology in the control group (Fig. 1A). However, several alterations such as aneurysm, epithelial cell hyperplasia, edema, displacement of epithelial cells, chloride cell hyperplasia, complete fusion of lamellae, telangiectasia and necrosis are observed in the PM treatment group (Fig. 1B). These results are in good agreement with a previous study of Borges and Pereira (2019). A recent study reported that goblet cells, mucin layer, and cell density confirmed that Korean diesel particulate matter (KDP20) exposure caused damage to the tissue and mucosal layer of zebrafish olfactory organs. In addition, recovery was confirmed to be possible in a clean environment without KDP20 (Song et al., 2022).

Ultrastructural changes in zebrafish gills

In the control group, multilayered epithelia covered gill filaments with pavement cells (PVCs) and undifferentiated basal cells (BCs) originated from the innermost layer in contact with the basal lamina are clearly visible. Cytoplasm filled with numerous electron-clear granules containing rounded mucous cells (MCs) is largely distributed along the margin of the filaments. Large-scale rounded or ovoid chloride cells (CCs) which are referred as mitochondria-rich cells are distributed on the inter lamellar region in a cluster fashion. These cells are associated with numerous mitochondria having a complicated tubular system. The modified endothelial cells, known as pillar cells (PCs) and macrophage-like cells (PMo) are clearly differentiated (Fig. 5A).

However, in the PM treatment group, the distorted outermost epithelial layer with detached external layer from the basal layer below

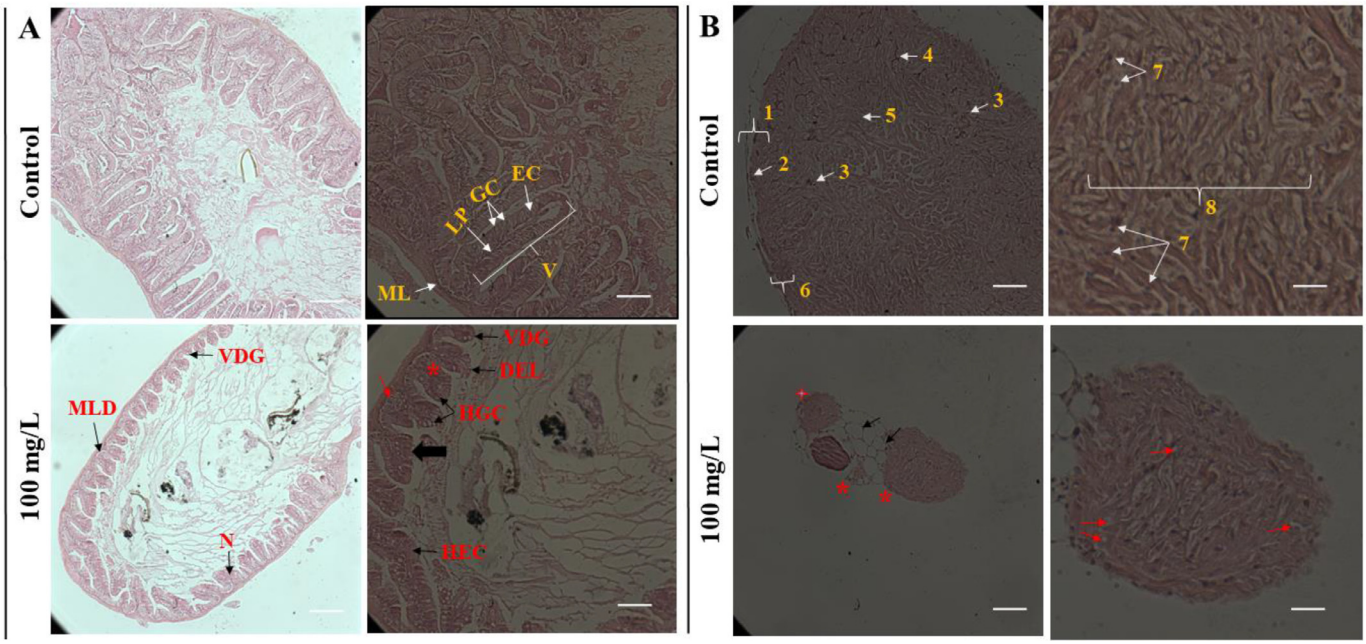

Fig. 2. Histopathological sections of the intestine and heart of female zebrafish stained with H&E. **(A)** The control intestine shows villi (V), lamina propria (LP), goblet cells (GC), enterocytes (EC) and muscle layer (ML) (top side images). The $PM_{2.5}$ (100 mg/L) treated intestine exhibits villi degeneration (VDG), detachment of the epithelium (DEL), hyperplasia of goblet cells (HGC), hypertrophy of enterocytes (HEC), muscle layer degeneration (MLD), necrosis (N), blood cell infiltrate (red arrow), fusion of the villi (thick black arrow) and eosinophils in the intestinal villi (asterisks) (bottom side images). **(B)** The control heart shows epicardium (1), coronary capillary (2), endocardium (3), intramyocardial capillary (4), fibroblastic tissue (5), coronary blood vessel (6), cardiomyocytes (7) and myocardium (8) (top side images). The $PM_{2.5}$ treated heart exhibits epicardial infiltration with lymphocytes, plasma cells and macrophages (asterisks), degeneration of coronary blood vessel (black arrows), unaltered blood vessels and epicardium (star) and intracellular vacuolization of myocardium-oedematous (red arrows) (bottom side images). Scale bar denotes 240 μm.

the wide lacunae is evident. In addition, PVCs show a sign of degeneration. Moreover, the ultrastructural arrangement demonstrates the disappearance of PMo cells and concomitant, degeneration of CCs. The BCs, PCs, CCs and erythrocytes still maintain their typical ultrastructural arrangement in the control group, while they are almost degenerated in the treatment group (Fig. 5B). After the exposure to mercury chloride, similar ultrastructural changes in zebrafish gills were reported by Macirella & Brunelli (2017). The exposure to fungicide tebuconazole also exerted an along effect on zebrafish gills (Macirella et al., 2018). The morphological changes appeared by $PM_{2.5}$ exposure include epithelial proliferation, ectopia of chloride cells, lamellar shortening, necrosis, and apoptosis. Interestingly, the apical and basal regions of lamellae in Nile tilapia showed different responses to the exposed copper (Monteiro et al., 2012). The apical region exhibited higher resistance to the toxic material compared to its counterpart.

Histopathological changes observed in zebrafish liver

Even though its structure is quite different with respect to physiological processes the zebrafish liver matches with mammalian system. In addition, it is the only dedicated site in the body for bile synthesis and it also performs the synthesis of lipids and vitellogenin (Goksøyr, 1995). After the exposure to toxic substances, the histopathology of zebrafish liver was compared to that of mammals (Vliegenthart et al., 2014).

Moreover, liver is a vital organ for detoxification in animals and it is involved in many physiological processes. In this study, the exposure of $PM_{2.5}$ to female zebrafish liver induced several alterations, such as hepatic plate gap (HPG), nucleus atrophy and necrosis of hepatocytes (NA&N), hyperemia (HY), vacuolization (V), nucleus vacuolization (NV), nucleus hypertrophy (NH) and cellular degeneration (CD) (Fig. 1B). The liver of control zebrafish group shows normal morphology (Fig. 1B). A previous study indicated that long-term accumulation of $PM_{2.5}$ drastically affected in attaining normal fish body weight. Similarly, the lipid droplets in the liver of the treatment groups were much smaller in size and less in number as compared to the control group (Zhao et al., 2021). $PM_{2.5}$ accumulation induces inflammation and oxidative stress in the liver by over expression of inflammation related genes and increased release of antioxidant enzymes (Morishita et al., 2004; Pu et al., 2018).

In addition, some compounds were reported to affect lipid metabolism inside the liver by changing lipid droplet percentage (Lai et al., 2018; Xiong et al., 2019; Zhou et al., 2019). According to Zhang et al. (2018) $PM_{2.5}$ decreases cell to cell contacts within the zebrafish liver tissue. Likewise, our previous findings also in support of the ill effects of $PM_{2.5}$ accumulations in zebrafish larvae (Manjunatha et al., 2021). As liver is an excellent bio-indicator of toxic substances specially of aquatic nature this should be considered as one of the sensitive and at the same time accurate parameter to evaluate the effects of toxic pollutants in aquatic bodies (Figueiredo-Fernandes et al., 2007).

Ultrastructural changes observed in zebrafish liver

Transmission electron microscopy (TEM) images of adult zebrafish liver revealed that hepatocytes were mostly polygonal in shape and they were assembled in a rather compact way with relatively rare sinusoids (Sn) in between. In addition, normal mitochondria (M), endothelial cell (En), cell nuclei (N), cell membrane and organelle structures in the control group were remained intact (Fig. 6A). Except the cristal swelling in individual mitochondria, no other lesions were observed in the $PM_{2.5}$exposed group. Zebrafish liver was mainly composed of hepatocytes in oval or polygonal shape, which form a rather compact structure interspersed with irregular sinusoids. Some hepatocytic organelles were dissolved and their contours were unclear. In addition, the endoplasmic reticulum was expanded, swollen, and fractured, and autophagosomes were existence. Glycogen profiles were occupied and fragments of digested erythrocytes were observed, as illustrated in

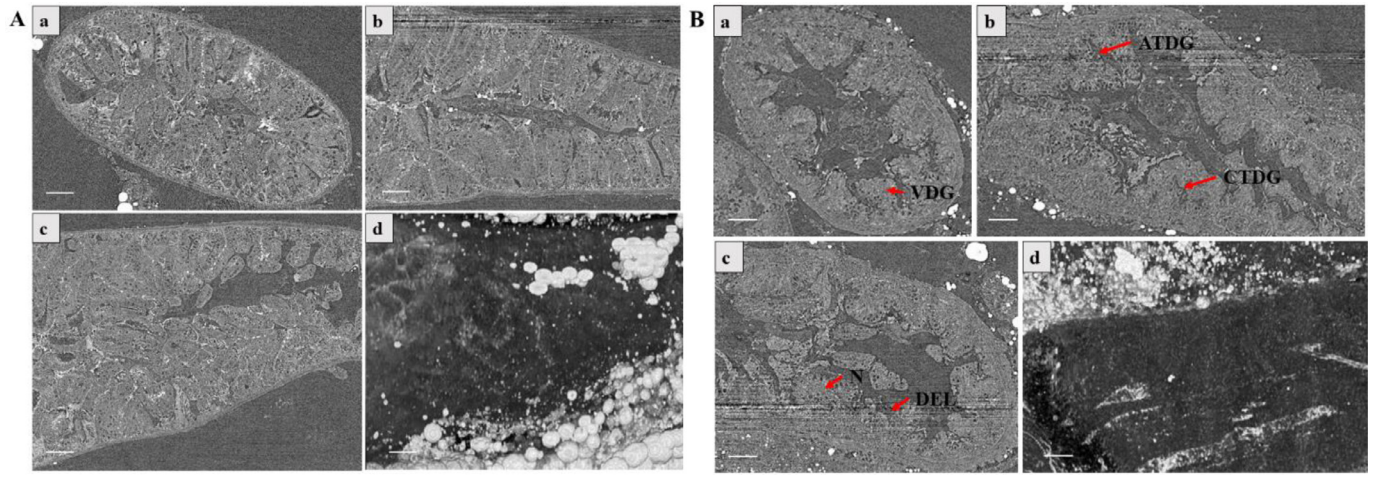

Fig. 3. X-ray micro CT images showing the intestines of female zebrafishes in the control **(A)** and 100 mg/L $PM_{2.5}$ treatment groups **(B)**. The control group shows normal intestine structures. The $PM_{2.5}$ treated group exhibits the presence of villi degeneration (VDG), detachment of epithelium (DEL), adipose tissue degeneration (ATDG), collagenous tissue degeneration (CTDG) and necrosis (N). Scale bar denotes 100 μm. Note: The image captured in different angle (a) XY- angle (b) YZ- angle, (c) XZ- angle and (d) 3D - image.

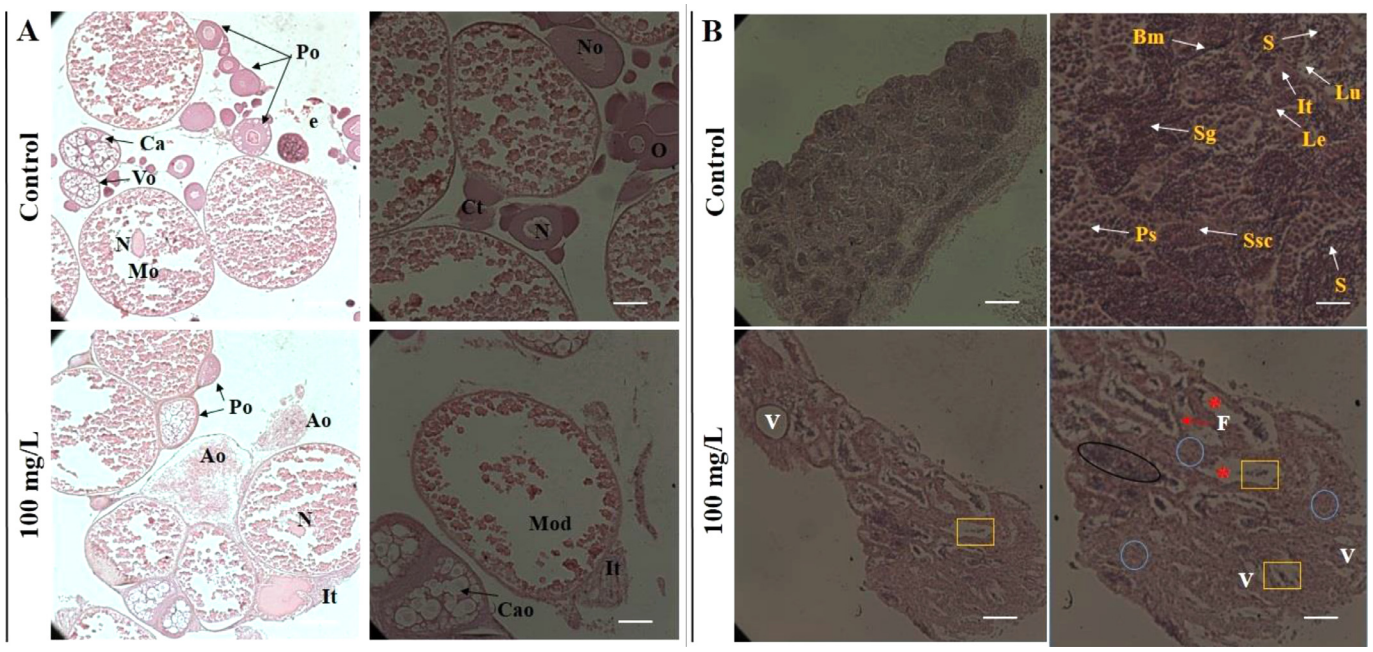

Fig. 4. Histopathological sections of the zebrafish gonads stained with H&E. **(A)** The control ovaries show nucleus (N), nucleus ooplasm (No), ooplasm (O), primary oocytes (Po), cortical alveoli (Ca), vitellogenic oocytes (Vo), connective tissue (Ct), mature oocytes (Mo) and erythrocyte (E) (top side images). The $PM_{2.5}$ (100 mg/L) treated ovaries exhibits atretic oocyte (Ao), nucleus membrane damage (N), interstitial tissue (It), cortical alveolus oocytes (Cao) and mature oocytes deformation (Mod) (bottom side images). **(B)** The control testis shows spermatogonium cells (Sg), primer spermatocytes (Ps), secondary spermatocyte cells (Ssc), sperm cells (S), basement membrane (Bm), luminal area (Lu), interstitial tissue (It) and leydig cells (Le) (top side images). The $PM_{2.5}$ (100 mg/L) treated testis exhibits degenerated spermatogenic cell clusters (encircled), separations between the sperms and other developing spermatogenic cell clusters (asterisks), hemorrhage in the intertubular area (arrowheads), vacuolization (V), decreased sperm cells (Squares), fibrosis (F) and fusion of some seminiferous tubules (ellipse) (bottom side images). Scale bar denotes 240 μm.

Fig. 6B. Similarly, Zhang et al. (2018) reported that the zebrafish treated with $PM_{2.5}$ showed significant structural abnormalities in hepatocytes. For example, the liver cell organelles were dissolved, and the vacuoles and many autophagosomes were found in the cytoplasm. In addition, hepatocytic organelles in the zebrafish larvae were also damaged by exposing to other pollutant of drug isoniazid (Zhang et al., 2019).

Histopathological changes in zebrafish intestine

$PM_{2.5}$ has remarkable histological impacts on the intestine of female zebrafish, such as villi degeneration (VDG), detachment of epithelia (DEL), hyperplasia of goblet cells (HGC), hypertrophy of enterocytes (HEC), muscle layer degeneration (MLD), necrosis (N), blood cell infiltrate (red arrow), fusion of villi (thick black arrow) and eosinophils in the intestinal villi (asterisks) (Fig. 2B). However, no change was observed in the control group (Fig. 2A). Similarly, X-ray micro CT images of intestine of the treated female zebrafish group show the presence of VDG, DEL, N, adipose tissue degeneration (ATDG), and collagenous tissue degeneration (CTDG), compared to the control group (Fig. 3).

$PM_{2.5}$ accumulations inside the marine medaka seriously affected gut microbiome, responsible for impaired lipid metabolism and suppressed growth (Zhao et al., 2021). In another study $PM_{2.5}$-treated zebrafish lar-

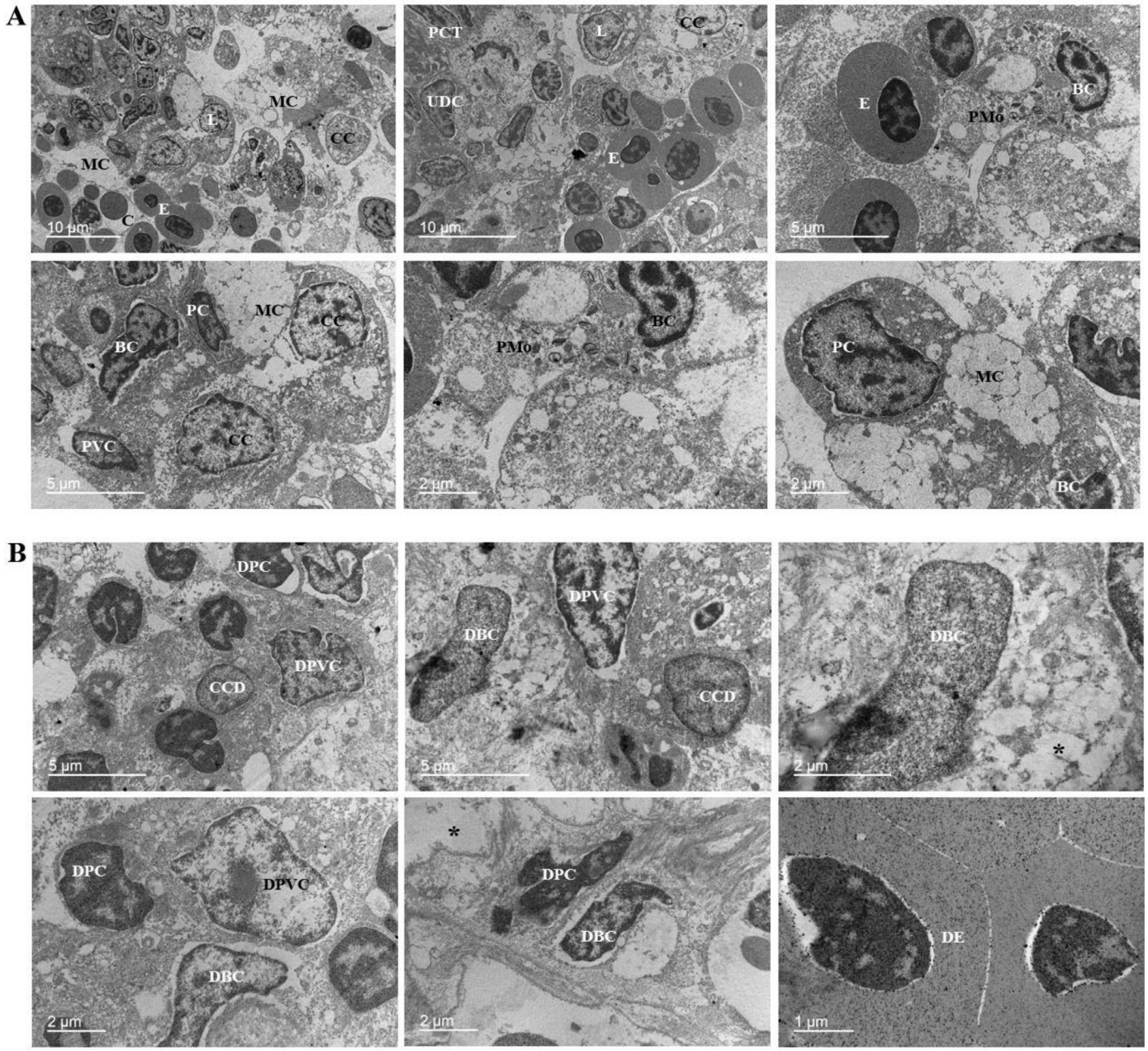

Fig. 5. Ultrastructures of the gills of female zebrafish in the control **(A)** and 100 mg/L $PM_{2.5}$ treatment groups **(B)**. The control gills show normal pavement cells (PVCs), basal cells (BCs), mucous cells (MCs), chloride cells (CCs), pillar cells (PCs), and precursors of macrophage-like cells (PMo). The $PM_{2.5}$ treated gills exhibit the enlargement of the tubular–vesicular system (asterisks), degeneration of pillar cells (DPC) and chloride cells (CCD), degeneration of pavement cells (DPVC) and basal cells (DBC), and detachment of erythrocytes (DE).

vae displyed frayed gut villi with weak intestinal walls (Zhang et al., 2018). In addition, perfluorooctane sulfonate (PFAS) and sodium p-perfluorous nonenoxybenzene sulfonate (OBS) both can affect intestinal fold height and also induces striated muscle cell necrosis (Huang et al., 2021).

Ultrastructural changes in zebrafish intestine

The present ultrastructural study revealed the presence of VDG, DEL, ATDG, CTDG and N in the intestine of the $PM_{2.5}$-treated zebrafish (Fig. 7A). However, the intestine of the control zebrafish shows normal structure (Fig. 7B). Most of the previous studies were based on the histological observations which were considered as direct inferences (Roberts and Ellis, 2012). But recent studies trying to establish a correlation between histology and physiology of the respective organ. (Borges et al., 2018; Carvalho et al., 2017; Takashima and Hibiya, 1984).

Histopathological changes in zebrafish heart

The histological studies on the heart of female zebrafish show normal epicardium (1), coronary capillary (2), endocardium (3), intramyocardial capillary (4), fibroblastic tissue (5), coronary blood vessel (6), cardiomyocyte (7) and myocardium (8) in the control group (Fig. 2B). Although the $PM_{2.5}$ treated zebrafish heart shows abnormal changes in epicardial infiltration with lymphocytes, plasma cells and macrophages (asterisks), degeneration of the coronary blood vessel (black arrows), unaltered blood vessels and epicardium (star) and intracellular vacuolization of the myocardium-oedematous (red arrows)

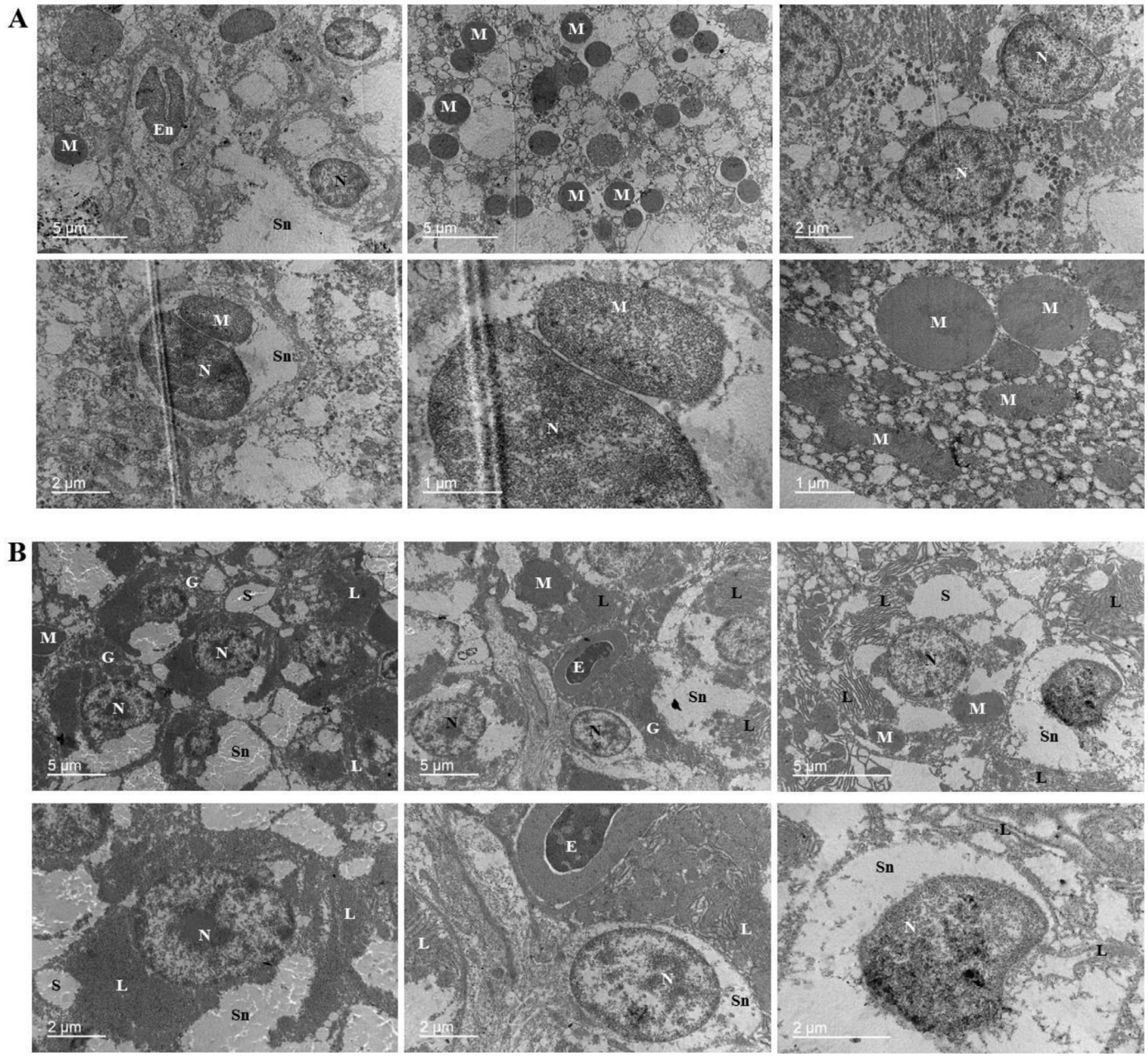

Fig. 6. Ultrastructures of the liver of female zebrafish in the control **(A)** and 100 mg/L $PM_{2.5}$ treatment groups **(B)**. The control liver shows normal mitochondria (M), endothelial cell (En), sinusoids (Sn) and cell nuclei (N). The $PM_{2.5}$ treated liver exhibits swollen mitochondria (M), rough endoplasmic reticulum (L), irregular sinusoids (Sn), cell nuclei (N), autophagosomes (S), glycogen (G) and erythrocyte (E).

(Fig. 2B). Zhang et al. (2018) reported that the exposure of $PM_{2.5}$ could impact on the heart tissues, for example, the myocardial layers and cells were decreased when zebrafish was exposed to 300 and 400 µg/mL $PM_{2.5}$. Our previous study also revealed the similar effect in the $PM_{2.5}$-exposed zebrafish model (Manjunatha et al., 2021).

Histopathological changes of zebrafish gonads

Compared to the control group, remarkably changes in atretic oocyte (Ao), nucleus membrane damage (N), interstitial tissue (It), cortical alveolus oocytes (Cao) and mature oocytes deformation (Mod) were observed in the ovary of the $PM_{2.5}$ treated female zebrafish (Fig. 4A). In the male testis of treated group, compared to the control group, remarkably variations in degenerated spermatogenic cell clusters (encircled), separation between the sperms and other developing spermatogenic cell clusters (asterisks), hemorrhage in the intertubular area (arrowheads), vacuolization (V), decreased sperm cells (Squares), fibrosis (F) and fusion of some seminiferous tubules (ellipse) were observed (Fig. 4B). The qualitative evaluation of this study evidenced some structural modifications in the treatment zebrafish group, comparing to the control group. Very limited studies have been performed in this field so far to evaluate the effect of $PM_{2.5}$ exposure on aquatic organisms. According to Yang et al. (2017) 1 mg/L of bisphenol F (BPF) is sufficient to induce reproductive impairments in zebrafish larvae. Furthermore, deltamethrin of different concentration exposure increases apoptosis in ovary and testis (Petrovici et al., 2020).

The concentrations of $PM_{2.5}$ exposed to zebrafish used in this study are rather lower than the realistic exposure scenarios for adult zebrafish. Therefore, the present results must be interpreted with caution. In the

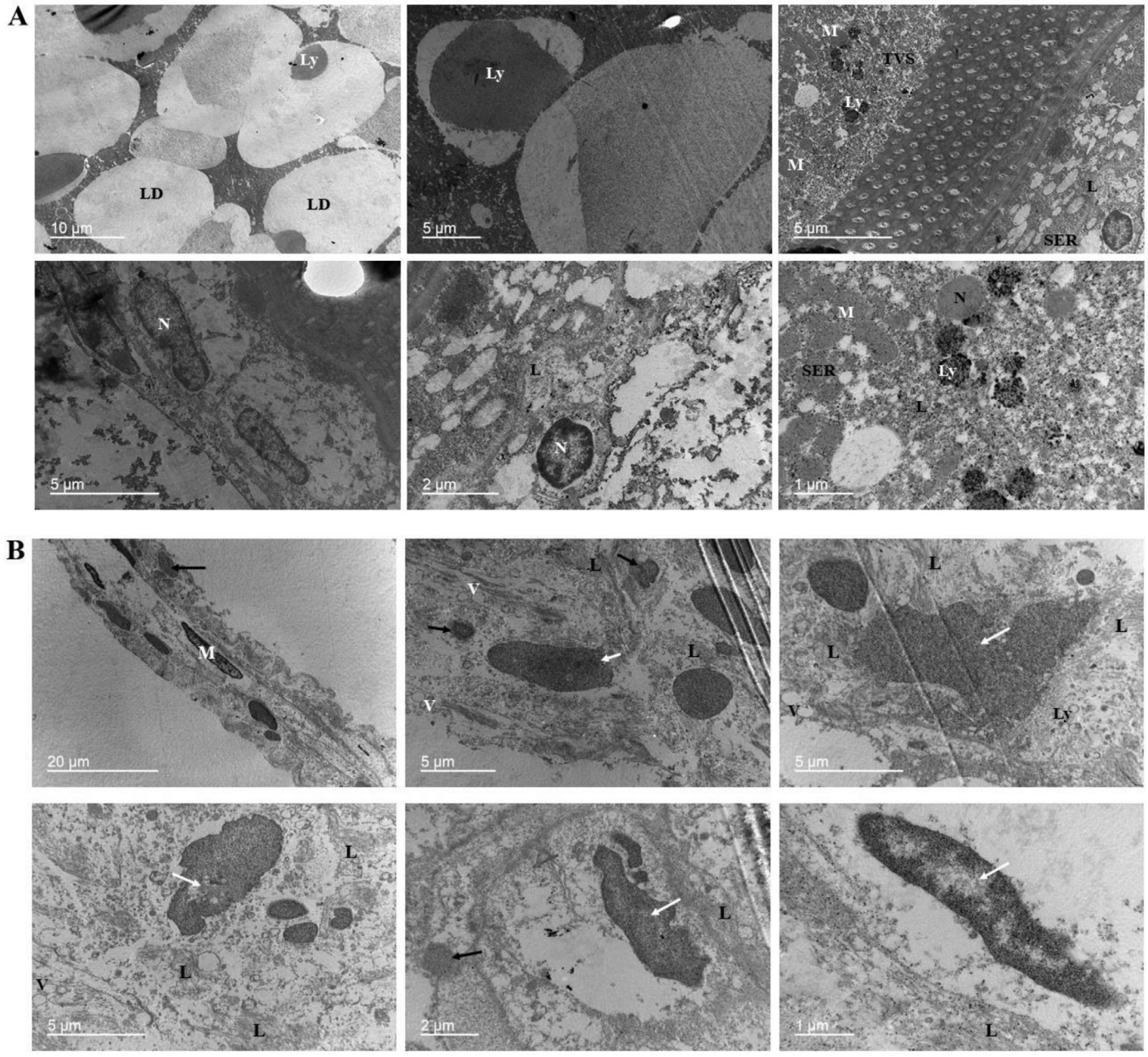

Fig. 7. Ultrastructures of the intestine of female zebrafish in the control **(A)** and 100 mg/L $PM_{2.5}$ treatment groups **(B)**. The control intestine shows normal lipid droplets (LD), smooth endoplasmic reticulum (SER), rough endoplasmic reticulum (L), lysosomes (Ly), mitochondria (M), nucleus (N) and gastric gland showing the tubulo-vesicular system (TVS). The $PM_{2.5}$ treated intestine exhibit the presence of vacuoles (V), Lysosomes (Ly) and chylomicrons enclosed by a membrane (black arrow), and some chylomicrons are observed between adjacent cells (white arrow). The rough endoplasmic reticulum is distended with desquamation of ribosome particles (L), mitochondria (M), nucleus (N) and abundant pynocitotic invaginations (red arrows).

histological and ultrastructural points of view, multi-organs (gills, liver, intestine, heart and gonads) of zebrafish revealed that the exposure of $PM_{2.5}$ could cause moderate to severe alterations in the treated zebrafish. Further, a molecular approach is very much warranted to unravel the mechanism behind the underlying physiological inferences of the study.

Conclusions

The present study demonstrated the importance of histopathological analysis as a useful biomarker in the assessment of $PM_{2.5}$ toxicity which menaces the quality of aquatic environment. In this study, the histopathology and ultrastructural morphological analysis using X-ray micro CT were comprehensively examined to evaluate the adverse effects of $PM_{2.5}$ on zebrafish model. The exposure of $PM_{2.5}$ was observed to affect the morphological structures of multi-organs (gill, liver, intestine, heart and gonads) and suppress the growth of zebrafish. Specifically, obvious changes were observed after the exposure of $PM_{2.5}$ in intestine images of X-ray micro CT. Additionally, when typical ultrastructural arrangements of multi-organs (gill, liver and intestine) were observed, their contours were indistinct, and organelles were melted, necrotized and fragmented in the treated zebrafish group. These results support that the air pollution associated with PM particles can elicit the ecological risk to aquatic organisms and humans. Moreover, the present

results would be particularly useful for future studies aiming to enhance basic knowledge on the developmental origins of epidemiological diseases.

This study clearly demonstrated that the exposure to $PM_{2.5}$ can induce histological and ultrastructural alterations in zebrafish. The present findings can be utilized to supplement the existing information on $PM_{2.5}$ toxicity. In addition, the histological and ultrastructural alterations are found to be used as sensitive biomarkers in the risk assessment of $PM_{2.5}$. Given the continuous exposure of $PM_{2.5}$ to natural aquatic environment in future studies, the potential toxic consequences of the long-term $PM_{2.5}$ exposure on fishes and humans would be warranted.

CRediT authorship contribution statement

Bangeppagari Manjunatha: investigation, visualization, conceptualization, methodology, validation, formal analysis, writing original draft and editing, funding acquisition. **Eunseok Seo**: samples pretreatment for X-ray micro CT and TEM analysis. **Deekshitha Bangyappagari**: formal analysis and writing – original draft. **Sang Joon Lee**: project administration, original draft editing, funding acquisition. All authors read and approved the final manuscript.

Declaration of Competing Interest

The authors declare that they have no known competing financial interests or personal relationships that could have appeared to influence the work reported in this paper.

Acknowledgement

The present study was supported by the Korea Research Fellowship (Brain Pool Program) through the National Research Foundation of Korea (NRF) funded by the Ministry of Science and ICT (grant no. 2016H1D3A1938252).

Supplementary materials

Supplementary material associated with this article can be found, in the online version, at doi:10.1016/j.hazadv.2022.100135.

References

Ali, S., Champagne, D.L., Spaink, H.P., Richardson, M.K., 2011. Zebrafish embryos and larvae: a new generation of disease models and drug screens. Birth Defects Res. Part C 93, 115–133.

Borges, R.S., & Pereira, A.C.M. (2019). Histopathology of zebrafish (*Danio rerio*) in non-clinical toxicological studies of new drugs. doi:10.5772/intechopen.88639.

Borges, R.S., Keita, H., Sanchez-Ortiz, B.L., Sampaio, T.I.S., Ferreira, I.M., Lima, E.S., Silva, M.J.A., Fernandes, C.P., Oliveira, A.E.M.F.M., Conceição, E.C., Rodrigues, A.B.L., Filho, A.C.M.P., Castro, A.N., Carvalho, J.C.T., 2018. Anti-inflammatory activity of nanoemulsions of essential oil from Rosmarinus officinalis L. In vitro and in zebrafish studies. Inflammopharmacology 26, 1057–1080.

Burgan, O., Smargiassi, A., Perron, S., Kosatsky, T., 2010. Cardiovascular effects of sub–daily levels of ambient fine particles: a systematic review. Environ. Health 9, 26.

Campagna, A.F., Fracacio, R., Rodrigues, B.K., Eler, M.N., Fenerich-Verani, N., Espindola, E.L.G., 2008. Effects of the copper in the survival, growth and gill morphology of *Danio rerio* (Cypriniformes, Cyprinidae). Acta Limnologica Brasiliensia 20, 253–259.

Carey, I.M., Atkinson, R.W., Kent, A.J., van Staa, T., Cook, D.G., Anderson, H.R., 2013. Mortality associations with long-term exposure to outdoor air pollution in a national English cohort. Am. J. Respir. Crit. Care Med. 187, 1226–1233.

Carvalho, J.C.T., Keita, H., Santana, G.R., de Souza, G.C., dos Santos, I.V.F., Amado, J.R.R., Kourouma, A., Prada, A.L., Carvalho, H.O., Silva, M.L., 2018. Effects of bothrops alternatus venom in zebrafish: a histopathological study. Inflammopharmacology 17, 273–284.

Carvalho, J.C.T., Keita, H., Santana, G.R., Souza, G.C., Santos, I.V.F., Amado, J.R.R., Kourouma, A., Prada, A.L., Carvalho, H.O., Silva, M.L., 2017. Effects of bothrops alternatus venom in zebrafish: a histopathological study. Inflammopharmacology 25, 273–284.

Cassar, S., Adatto, I., Freeman, J.L., Gamse, J.T., Iturria, I., Lawrence, C., Muriana, A., Peterson, R.T., Van Cruchten, S., Zon, L.I., 2020. Use of zebrafish in drug discovery toxicology. Chem. Res. Toxicol. 33, 95–118.

Chew, S., Kolosowska, N., Saveleva, L., Malm, T., Kanninen, K.M., 2020. Impairment of mitochondrial function by particulate matter: implications for the brain. Neurochem. Int. 135, 104694.

Chhetri, J., Jacobson, G., Gueven, N., 2014. Zebrafish—On the move towards ophthalmological research. Eye 28, 367–380.

Chuang, K.J., Chan, C.C., Su, T.C., Lee, C.T., Tang, C, S, 2007. The effect of urban air pollution on inflammation, oxidative stress, coagulation, and autonomic dysfunction in young adults. Am. J. Respir. Crit. Care Med. 176, 370–376.

Darrow, L.A., Klein, M., Flanders, W.D., Mulholland, J.A., Tolbert, P.E., Strickland, M.J., 2014. Air pollution and acute respiratory infections among children 0 –4 years of age: an 18 – year time-series study. Am. J. Epidemiol. 180, 968–977.

Delfino, R.J., Staimer, N., Tjoa, T., Gillen, D.L., Polidori, A., Arhami, M., Kleinman, M.T., Vaziri, N.D., Longhurst, J., Sioutas, C., 2009. Air pollution exposures and circulating biomarkers of effect in a susceptible population: clues to potential causal component mixtures and mechanisms. Environ. Health Perspect. 117, 1232–1238.

Dooley, K., Zon, L.I., 2000. Zebrafish: a model system for the study of human disease. Curr. Opin. Genet. Dev. 10, 252–256.

Du, Y., Xu, X., Chu, M., Guo, Y., Wang, J., 2016. Air particulate matter and cardiovascular disease: the epidemiological, biomedical and clinical evidence. J. Thorac. Dis. 8, E8–E19.

Figueiredo-Fernandes, A., Ferreira-Cardoso, J.V., Garcia-Santos, S., Monteiro, S.M., Carrola, J., Matos, P., Fontaínhas-Fernandes, A., 2007. Histopathological changes in liver and gills epithelium of Nile tilapia, *Oreochromis niloticus* exposed to waterborne copper. Pesqui. Vet. Bras. 27, 103–109.

Fu, Q., Lyu, D., Zhang, L., Qin, Z., Tang, Q., Yin, H., Lou, X., Chen, Z., Yao, K., 2017. Airborne particulate matter ($PM_{2.5}$) triggers autophagy in human corneal epithelial cell line. Environ. Pollut. 227, 314–322.

Goksøyr, A., 1995. Use of cytochrome P450 lA (CYP1A) in fish as a biomarker of aquatic pollution. Arch. Toxicol. Suppl. 17, 80–95.

Holden, J.A., Lester, J.L., Matthews, J.L., 2012. In: The zebrafish: Atlas of Macroscopic and Microscopic Anatomy, 86. Cambridge University Press, Cambridge, UK, p. 147.

Hu, F., Guo, Y., 2021. Health impacts of air pollution in China. Front. Environ. Sci. Eng. 15, 74.

Hu, W., Downward, G.S., Reiss, B., Xu, J., Bassig, B.A., Hosgood 3rd, H.D., Zang, L., Seow, W.J., Wu, G., Champman, R.S., Tian, L., Wei, F., Vermeulen, R., Lan, Q., 2014. Personal and indoor $PM_{2.5}$ exposure from burning solid fuels in vented and unvented stoves in a rural region of China with a high incidence of lung cancer. Environ. Sci. Technol. 48, 8456–8464.

Huang, J., Wang, Q., Liu, S., Zhang, M., Liu, Y., Sun, L., Wu, Y., Tu, W., 2021. Crosstalk between histological alterations, oxidative stress and immune aberrations of the emerging PFOS alternative OBS in developing zebrafish. Sci. Total Environ. 774, 145443.

Karlsson, L., 1983. Gill morphology in the zebrafish, *Brachydanio rerio* (Hamilton-Buchanan). J. Fish Biol. 23, 511–524.

Lai, Y., Zhou, C., Huang, P., Dong, Z., Mo, C., Xie, L., Lin, H., Zhou, Z., Deng, G., Liu, Y., Chen, Y., Huang, S., Wu, Z., Sun, X., Gao, L., Lv, Z., 2018. Polydatin alleviated alcoholic liver injury in zebrafish larvae through ameliorating lipid metabolism and oxidative stress. J. Pharmacol. Sci. 138, 46–53.

Lee, B.J., Kim, B., Lee, K., 2014. Air pollution exposure and cardiovascular disease. Toxicol Res 30, 71–75.

Lee, S.J., Kim, H.N., Choi, W., Yoon, G.Y., Seo, E., 2019. A nature-inspired lubricant-infused surface for sustainable drag reduction. Soft. Matter 1, 8459–8467.

Lelieveld, J., Evans, J.S., Fnais, M., Giannadaki, D., Pozzer, A., 2015. The contribution of outdoor air pollution sources to premature mortality on a global scale. Nature 525, 367–371.

Li, T., Hu, R., Chen, Z., Li, Q., Huang, S., Zhu, Z., Zhou, L.F., 2018. Fine particulate matter ($PM_{2.5}$): the culprit for chronic lung diseases in China. Chronic Dis. Trans. Med. 4, 176–186.

Lippi, G., Favaloro, E.J., Franchini, M., Guidi, G.C., 2008. Air pollution and coagulation testing: a new source of biological variability? Thromb. Res. 123, 50–54.

Lu, F., Xu, D., Cheng, Y., Dong, S., Guo, C., Jiang, X., Zheng, X., 2015. Systematic review and meta-analysis of the adverse health effects of ambient $PM_{2.5}$ and PM_{10} pollution in the Chinese population. Environ. Res. 136, 196–204.

Macirella, R., Brunelli, E., 2017. Morphofunctional alterations in zebrafish (*Danio rerio*) gills after exposure to mercury chloride. Int. J. Mol. Sci. 18, 824.

Macirella, R., Tripepi, M., Brunelli, E., 2018. Morphological and immunohistochemical modifications in zebrafish (*Danio rerio*) gills after short-term exposure to the fungicide tebuconazole. Zebrafish 1638.

Manjunatha, B., Philip, G.H., 2016. Reproductive toxicity of chlorpyrifos tested in zebrafish (*Danio rerio*): histological and hormonal end points. Toxicol. Ind. Health 32, 1808–1816.

Manjunatha, B., Deekshitha, B., Seo, E., Kim, J., Lee, S.J., 2021. Developmental toxicity induced by particulate matter ($PM_{2.5}$) in zebrafish (*Danio rerio*) model. Aquat. Toxicol. 238, 105928.

Mazon, A.F., Cerqueira, C.C.C., Fernandes, M.N., 2002. Gill cellular changes induced by copper exposure in the South American tropical freshwater fish *Prochilodus scrofa*. Environ. Res. 88, 52–63.

Meletti, P.C., 2016. Avaliação Da Degradação Ambiental Por Meio De Testes De Toxicidade Com Sedimento e De Análises Histopatológicas Em Peixes. Universidade de São Paulo, São Carlos Available from.

Monteiro, S.M., Oliveira, E., Fontaínhas-Fernandes, A., Sousa, M., 2012. Effects of sublethal and lethal copper concentrations on the gill epithelium ultrastructure of Nile tilapia, *Oreochromis niloticus*. Zool. Stud. 51, 977–987.

Morishita, M., Keeler, G., Wagner, J., Marsik, F., Timm, E., Dvonch, J., Harkema, J., 2004. Pulmonary retention of particulate matter is associated with airway inflammation in allergic rats exposed to air pollution in urban Detroit. Inhal. Toxicol. 16, 663–674.

Park, J., Park, E.H., Schauer, J.J., Yi, S.M., Heo, J., 2018. Reactive oxygen species (ROS) activity of ambient fine particles ($PM_{2.5}$) measured in Seoul, Korea. Environ. Int. 117, 276–283.

Petrovici, A., Strungaru, S.A., Nicoara, M., Robea, M.A., Solcan, C., Faggio, C., 2020. Tox-

icity of deltamethrin to zebrafish gonads revealed by cellular biomarker. J. Mar. Sci. Eng. 8, 73.
Pu, X.J., Li, J., Zhou, Q.L., Pan, W., Li, Y.Q., Zhang, Y., Wang, J., Jiao, Z., 2018. Rosiglitazone inhibits $PM_{2.5}$-induced cytotoxicity in human lung epithelial A549 cells. Ann. Transl. Med. 6, 152.
Rezende, K.F.O., Santos, R.M., Borges, J.C.S., Salvo, L.M., Da Silva, J.R.M.H.C, 2014. Histopathological and genotoxic effects of pollution on Nile tilapia (*Oreochromis niloticus*, Linnaeus, 1758) in the Billings reservoir (Brazil). Toxicol. Mech. Methods 24, 404–411.
Roberts, R.J., Ellis, A.E., 2012. The anatomy and physiology of teleosts. In: Fish Pathology. Philadelphia, PA, USA, pp. 12–54 Roberts, R.J., Ed.; W. B. Saunders2012.
Santos, D.C.M., Cupertino, M.C., Matta, S.L.P., Oliveira, J.A., Santos, J.A.D., 2015. Histological alterations in liver and testis of *Astyanax* aff. *bimaculatus* caused by acute exposition to zinc. Revista Ceres 62, 131–141.
Seo, E., Yoon, G.Y., Kim, H.N., Lim, J.H., Kim, S., Kim, B., Kim, K.H., Lee, S.J., 2020. Morphological features of mucous secretory organ and mucous secretion of loach *Misgurnus anguillicaudatus* skin for friction drag reduction. J. Fish Biol. 96, 83–91.
Song, C., He, J., Wu, L., Jin, T., Chen, X., Li, R., Ren, P., Zhang, L., Mao, H., 2017. Health burden attributable to ambient $PM_{2.5}$ in China. Environ. Pollut. 223, 575–586.
Song, S.J., Park, B., Jo, K., Kim, C.S., 2022. Damage to olfactory organs of adult zebrafish induced by diesel particulate matter. Int. J. Mol. Sci. 23, 407.
Takashima, F., Hibiya, T., 1984. An atlas of fish histology-normal and pathological features. Kodansha Ltd. Tóquio 69, 406.
Van Den Heuvel, M.R., Power, M., Richards, J., MacKinnon, M., Dixon, D.G., 2000. Disease and gill lesions in yellow perch (*Perca flavescens*) exposed to oil sands mining-associated waters. Ecotoxicol. Environ. Saf. 46, 334–341.
Vliegenthart, A.D., Tucker, C.S., Del Pozo, J., Dear, J.W., 2014. Zebrafish as model organisms for studying drug-induced liver injury. Br. J. Clin. Pharmacol. 78, 1217–1227.
Wang, J., Huang, J., Wang, L., Chen, C., Yang, D., Jin, M., Bai, C., Song, Y., 2017. Urban particulate matter triggers lung inflammation via the ROS-MAPK-NF-kappaB signaling pathway. J. Thorac. Dis. 9, 4398–4412.
Wang, Z., Du, J., Lam, S.H., Mathavan, S., Matsudaira, P., Gong, Z., 2010. Morphological and molecular evidence for functional organization along the rostrocaudal axis of the adult zebrafish intestine. BMC Genomics 11, 392.
Westerfield, M., 1995. The Zebrafish Book. In: A Guide For the Laboratory Use of Zebrafish (*Danio Rerio*). University of Oregon Press, Eugene, p. 385.
World Health Organization (WHO) (2018a) Ambient (outdoor) air quality and health. Accessed date: 1 August 2019.
World Health Organization (WHO) (2018b) Ambient (outdoor) air pollution and health. Accessed date: 5 April 2019.
World Health Organization (WHO) (2019) Ten threats to global health in 2019. Accessed date: 5 April 2019.
Xiong, F., Wu, S., Qin, L., Shi, M., Li, W., Zou, H., Li, M., Wang, G., 2019. Transcriptome analysis of grass carp provides insights into disease-related genes and novel regulation pattern of bile acid feedback in response to lithocholic acid. Aquaculture 500, 613–621.
Yang, B., Qian, Z., Howard, S.W., Vaughn, M.G., Fan, S., Liu, K., Dong, G.H, 2018. Global association between ambient air pollution and blood pressure: a systematic review and meta-analysis. Environ. Pollut. 235, 576–588.
Yang, Q., Yang, X., Liu, J., Ren, W., Chen, Y., Shen, S., 2017. Effects of BPF on steroid hormone homeostasis and gene expression in the hypothalamic–pituitary–gonadal axis of zebrafish. Environ. Sci. Pollut.n Res. 24, 21311–21322.
Zanobetti, A., Dominici, F., Wang, Y., Schwartz, J.D., 2014. A national case cross over analysis of the short-term effect of $PM_{2.5}$ on hospitalizations and mortality in subjects with diabetes and neurological disorders. Environ. Health 13, 38.
Zhang, Y., Cen, J., Jia, Z., Hsiao, C.-.D., Xia, Q., Wang, X., Chen, X., Wang, R., Jiang, Z., Zhang, L., Liu, K., 2019. Hepatotoxicity induced by isoniazidlipopolysaccharide through endoplasmic reticulum stress, autophagy, and apoptosis pathways in zebrafish. Antimicrob. Agents Chemother. 63 01639–18.
Zhang, Y., Li, S., Li, J., Han, L., He, Q., Wang, R., Wang, X., Liu, K., 2018. Developmental toxicity induced by $PM_{2.5}$ through endoplasmic reticulum stress and autophagy pathway in zebrafish embryos. Chemosphere 197, 611–621.
Zhao, P., Lu, W., Hong, Y., Chena, J., Dong, S., Huang, Q., 2021. Long-term wet precipitation of $PM_{2.5}$ disturbed the gut microbiome and inhibited the growth of marine medaka (*Oryzias melastigma)*. Sci. Total Environ. 755, 142512.
Zhou, C., Lai, Y., Huang, P., Xie, L., Lin, H., Zhou, Z., Mo, C., Deng, G., Yan, W., Gao, Z., Huang, S., Chen, Y., Sun, X., Lv, Z., Gao, L., 2019. Naringin attenuates alcoholic liver injury by reducing lipid accumulation and oxidative stress. Life Sci. 216, 305–312.
Zhou, M., Liu, Y., Wang, L., Kuang, X., Xu, X., Kan, H., 2014. Particulate air pollution and mortality in a cohort of Chinese men. Environ. Pollut. 186, 1–6.